European Research Infrastructure supporting Smart Grid and Smart Energy Systems Research, Technology Development, Validation and Roll Out – Second Edition

Project Acronym: **ERIGrid 2.0**

Project Number: **870620**

Technical Report Lab Access User Project

Assessing the Provision of a Multi-Ancillary Service Framework provided by PV-BES Systems (ProMiSe)

Access Duration: 28/11/2022 to 09/12/2022

Funding Instrument:	Research and Innovation Action
Call:	H2020-INFRAIA-2019-1
Call Topic:	INFRAIA-01-2018-2019 Integrating Activities for Advanced Communities
Project Start:	1 April 2020
Project Duration:	54 months

User Group Leader: Theofilos Papadopoulos (Democritus University of Thrace)

This project has received funding from the European Union's Horizon 2020 research and innovation programme under Grant Agreement No. 870620.

Report Information

Document Administrative Information	
Project Acronym:	ERIGrid 2.0
Project Number:	870620
Access Project Number:	149
Access Project Acronym:	ProMiSe
Access Project Name:	Assessing the Provision of a Multi-Ancillary Service Framework provided by PV-BES Systems
User Group Leader:	Theofilos Papadopoulos (Democritus University of Thrace)
Document Identifier:	ERIGrid2-Report-Lab-Access-User-Project-149-ProMiSe-draft-v1.1
Report Version:	v1.1
Contractual Date:	19/01/2023
Report Submission Date:	25/01/2023
Lead Author:	Kalliopi Pippi (Democritus University of Thrace)
Co-author(s):	Theofilos Papadopoulos (Democritus University of Thrace), Georgios Kryonidis (Aristotle University of Thessaloniki)
Keywords:	Ancillary services, voltage regulation, unbalance mitigation, three-phase four-leg converter, European Union (EU), H2020, Project, ERIGrid 2.0, GA 870620
Status:	1st draft

Change Log

Date	Version	Author/Editor	Summary of Changes Made
19/01/2023	v1.0	Kalliopi Pippi	Draft report template
23/01/2023	v1.1	Theofilos Papadopoulos	Updated version

Table of Contents

List of Figures

List of Tables

List of Abbreviations

3Ph4LC 3-phase 4-leg converter
ADN Active Distribution Network
AS Ancillary Services
CC Central Controller
DBES Distributed Renewable Energy Source
DN Distribution Network
DRES Distributed Renewable Energy Source
DSOs Distribution System Operators
LA Lab Access
LC Local Controller
LV Low-Voltage
MV Medium-Voltage
PHiL Power Hardware-in-the-Loop
POI Point of Interconnection
PVs Photovoltaics
RTDS Real Time Digital Simulator
UG User Group
UP User Project
VR Voltage Regulation
VUM Voltage Unbalance Mitigation

Executive Summary

Scope of this technical report is to briefly present the main remarks drawn in ProMiSe project. In particular, scope of ProMiSe is to test and validate a new unified control architecture used to overcome voltage violation and voltage unbalance issues utilizing a power hardware-in-the-loop platform.

1 Lab-Access User Project Information

1.1 Overview

The main information regarding the Lab-Access User Project (UP) and the user group (UG) are summarized in Tables 1 and 2, respectively.

Table 1: UP main information

UP Title	Assessing the Provision of a Multi-Ancillary Service Framework provided by PV-BES Systems
UP Acronym	ProMiSe
Host Laboratory	Dynamic Power Systems Laboratory (UST)

Table 2: UG main information

Name	Role	Physical Access
Theofilos Papadopoulos	Leader	YES
Kalliopi Pippi	Member	YES
Georgios Barzegkar-Ntovom	Member	NO
Georgios Kryonidis	Member	YES
Eleftherios Kontis	Member	NO

1.2 Research Motivation, Objectives, and Scope

The advent of distributed renewable energy sources (DRESs) has led to a series of technical issues affecting the secure and reliable operation of active distribution networks (ADNs). Among them under-/overvoltages and voltage unbalance can be considered as two of the most important problems limiting the increase of DRES penetration. ProMiSe introduces a new unified control architecture to overcome these issues and provide ancillary services (AS) by using the reactive power of DRESs and the active/reactive power of distributed battery energy storage systems (DBESs). A major feature is the implementation in the symmetrical components domain, allowing the efficient decoupling between under-/overvoltage and voltage unbalance mitigation techniques.

The proposed unified control strategy has been already validated in terms of time-domain and long-term quasi-static timeseries simulations in low- and medium-voltage networks. However, a thorough and detailed study, exceeding the technical boundaries of software simulation environments is required. Scope of this project is to test and validate the proposed unified control strategy utilizing a power hardware-in-the-loop (PHiL) platform. This validation scheme will reflect a range of different scenarios and realistic test cases of integration of the unified control strategy in modern distribution networks. The scale-up of these tests and their processing will offer a good insight on AS provision for the distribution system operator and our research team. Therefore, the main targets of ProMiSe are:

- to test the performance and the functionalities of the proposed unified control strategy in

a low-voltage (LV) distribution network (DN), consisting of loads and DRESs;

- to perform PHiL tests, to evaluate the performance of the proposed unified control strategy under real field conditions;
- to investigate the effect of network parameters, i.e., the *R*/*X* line ratio, on the performance of the provided AS.

1.3 Structure of the Document

This document is organised as follows: Section 2 briefly outlines the state-of-the-art that provides the basis of the realised Lab Access (LA) User Project (UP). Section 3 briefly outlines the performed experiments whereas Section 4 summarises the results and conclusions. Finally, potential open issues and suggestions for improvements are discussed in Section 5.

2 State-of-the-Art

Currently, the conventional passive DNs are gradually converted to active systems, due to the advent of DRESs, especially photovoltaics (PVs) [1]. This transition from the passive to active operation of DNs contributes to the development of new AS that can exploit the functionalities of network assets, e.g., DBES systems, DRES, etc., to tackle long-term power quality problems related to the steady operation of DNs [2]. **Voltage regulation (VR) and voltage unbalance mitigation (VUM)** are considered as two of the most important AS within the DN premise [3].

In literature, several solutions have been proposed to tackle **voltage violations**. More specifically, a consensus control scheme is presented in [4] where the active power of DBES is used to control network voltages. The use of the reactive power of DRESs and DBESs as the only means for VR is assessed in[5]. Nevertheless, the performance of this method is limited since it does not fully exploit the controllability potential that can be provided by the combined use of active and reactive power. This is addressed in [6] by proposing a decentralized, droop-based method where the active power of DBES is combined with the reactive power of DRES to control the network voltages. However, active power is prioritized against reactive power increasing the DBES utilization and deteriorating their lifetime expectancy. This priority is reversed in [7] where a consensus-based distributed control scheme is employed to coordinate the response of DRESs. Another promising solution is the use of centralized control schemes where the operating points of DRESs and DBESs are determined using optimization techniques [8], or rule-based [9] approaches. However, these methods assume balanced networks, which is unrealistic for LV DNs.

The **unbalanced grid operation** is considered in the VR algorithms developed in [10][12]. In particular, in [10], a consensus algorithm is proposed controlling the active power of DRESs and DBESs at each phase separately. A similar approach is presented in [11] where a distributed algorithm is employed to control the output power of DRESs and DBESs. A decentralized solution is presented in [12] where single-phase droop curves are introduced to tackle voltage violations. As a common drawback, these methods control the phase-to-neutral voltages which is not compliant with the regulation of the positive sequence voltage imposed by the recently revised IEEE 1547 Standard [13]. Additionally, a strong coupling between voltage unbalance and positive-sequence voltage is introduced, hindering the individual handling.

Considering VUM, an extended version of the Steinmetz design is proposed in [14] where the zero- and/or negative-sequence voltages at critical network nodes are eliminated by properly adjusting the re-active power of DRESs among the three-phases. Although this method is valid, continuous monitoring of the unbalanced loading conditions is needed, while the impact on the positive-sequence voltages is not assessed. In [15] and [16], an alternative VUM technique involves the use of the damping conductance concept enabling DRESs to behave as a constant shunt resistance in the zero- and negative sequence. Moreover, the damping conductance concept is combined with a droop curve to address potential overvoltages. However, the developed solution leads to conflicting objectives since there is a strong coupling between VR and VUM.

To overcome the above problems, our research team has developed a **unified control strategy for unbalanced LV distribution grids**, combining the distinct features of the above-mentioned categories. More explicitly, the proposed methodology coordinates two algorithms concerning VR and VUM. In the unified strategy DRESs and DBESs are used as the main control assets for providing AS to distribution system operators (DSOs) to solve local DN problems.

3 Executed Tests and Experiments

3.1 Test Plan, Standards, Procedures, and Methodology

The goal of ProMiSe is to perform testing and validation experiments concerning the applicability, feasibility and efficiency of the proposed unified control strategy to provide AS to unbalanced LV distribution grids by managing DRES-DBES systems. The proposed strategy coordinates two AS algorithms concerning VR and VUM. A hierarchical two-layer architecture is adopted and the distinct feature of the proposed strategy is that avoids coupling interactions among the control algorithms by implementing them in the symmetrical components domain. In particular, the VR method regulate the positive sequence voltages, while the VUM algorithm aims to reduce the zero- and the negative-sequence voltages. In such a manner the proposed VR becomes also compliant with the requirements posed by the IEEE 1547 Std. [13].

The proposed architecture is presented in Fig. 1 and consists of two distinct implementation layers [17]:

- The local controller (LC) layer. This layer corresponds to the design of a LC that can be integrated in grid-interfaced three-phase, four-leg converters (3Ph4LC) of DRESs/DBESs. Scope of the LC is to adjust the 3Ph4LC output power based only on the measurements acquired at the point of interconnection (POI) with the grid in order to address potential voltage violations and unbalances.
- The central controller (CC) layer. In this layer, a CC is employed to coordinate the control actions taken by the LCs. The aim of the coordination procedure is threefold: (a) to avoid possible interactions caused by the simultaneous triggering and interactions of LCs, (b) to identify LCs that should contribute towards a violation event and (c) perform a day-ahead planning to ensure that sufficient amount of energy will be available to be provided/stored by the DBES.

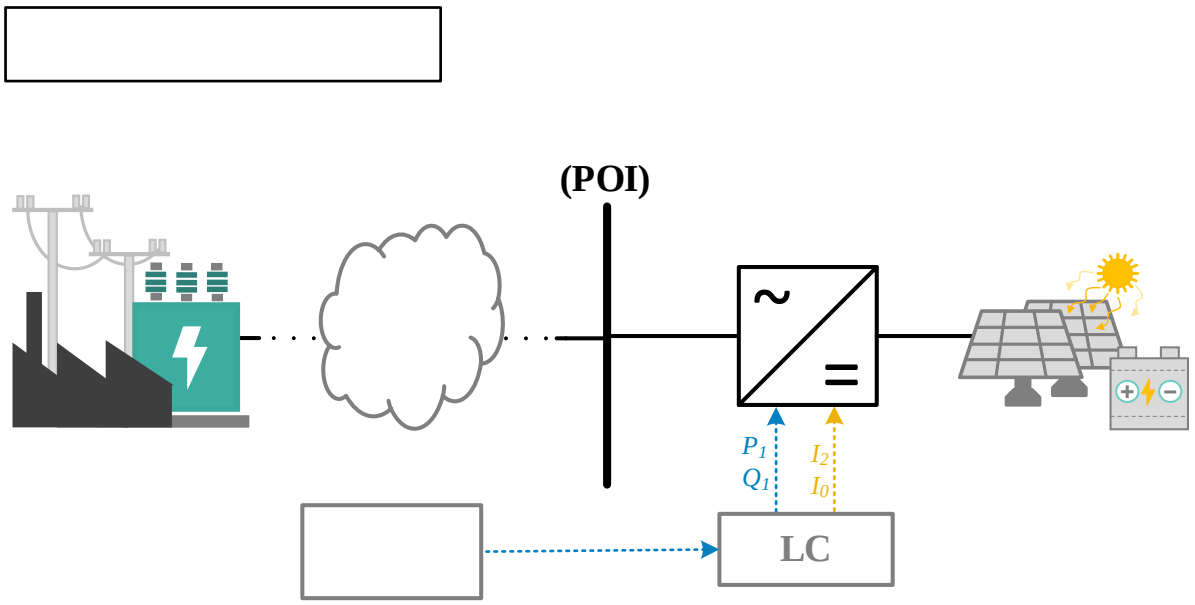

Figure 1: Control architecture of the proposed method.

A conceptual representation of the proposed unified strategy is depicted in Figure 2 and comprises two individual control blocks referred to the VR and VUM. The LC functionalities to provide VR and VUM are described briefly:

- According to the proposed VUM control strategy, voltage unbalance is mitigated by controlling the zero- and negative- sequence currents, I_0 and I_2, respectively. This assumption complies with early grid codes[1] that foresee grid converters to provide AS exploiting negative-sequence currents. The contribution of each unit to VUM is achieved by regulating the zero- and negative- sequence reactive power via damping susceptances Y_0 and Y_2, respectively.
- VR is achieved by controlling the positive-sequence network voltages, thus being in line with the IEEE 1547 Standard [13]. This is attained by controlling only the positive-sequence complex output power of DRESs/DBESs following a low-complexity procedure combining local measurements and information received from the CC. Towards this objective, a two-way communication channel is established between the central and LCs. For this operation, the use of reactive power is prioritized against the active power to ensure decreased DBES utilization.

More information regarding the employed VR and VUM control schemes can be found in [17].

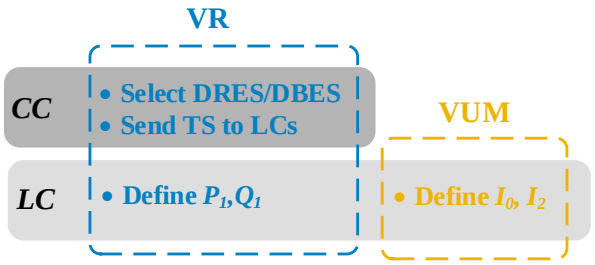

Figure 2: Conceptual representation of the proposed unified control strategy.

The proposed unified control strategy has been already validated in terms of time-domain and long-term quasi-static timeseries and simulations [17]. However, a thorough and **detailed grid integration study**, exceeding the technical boundaries of software simulation environments, utilizing a PHiL platform **is required**.

The PHiL technology provides full insight and intricate details of the effect of grid practical operating conditions (load variation, noise, harmonics, etc.), the real-time interactions with other assets (DRES converters with different control strategies, stability issues, etc.) and the realistic communications (delays, noise, etc.). Therefore, **the ultimate goal of ProMiSe** is to perform realistic test cases and validation procedures.

More specifically, the main features and targets of the proposed research project are:

- to test the performance and the functionalities of the proposed unified strategy in a LV DN, consisting of loads and DRESs;
- to model in the RTS, the LC embedded in a virtual LV 3Ph4LC that supports the proposed AS (VR, VUM). The LC will be considered connected at a specific node of the test system;
- to connection the LV power network of the laboratory in the developed LV DN. The LV power network will include: three-phase static load bank and a three-phase DRES type converter;
- to investigate the effect of network parameters, i.e., the *R*/*X* line ratio, on the performance of the provided AS;
- to compare the results considering a detailed converter model against a simplified approach.

[1] Vde-ar-n 4120, technical requirements for the connection and operation of customer installations to the high voltage network (tab high voltage) (2015).

3.2 Test Set-ups

During the lab visit, three experimental test cases have been tested:

- **Experiment 1** (Total Duration ~16min: duration of experiment (1min) + data acquisition (15min)): The performance of the proposed unified strategy is evaluated in the configuration of Figure 3. The LV DN, the detailed model of a 3Ph4LC (See Figure 4) and the VR/VUM algorithms are developed in the real time digital simulator (RTDS). Note that in order to have the full model of the 3Ph4LC the 'Small time step Library' of RSCAD program has been used. During the experiment, the following steps have been done:

  Step 1. AS remain deactivated (Duration 12s). At the beginning of the experiment an overvoltage event is observed at node 4, i.e., the node where the ProMiSe 3Ph4LC is located. Note that an overvoltage event is detected when the positive sequence voltage at the examined node exceeds 1.1pu. Recording of the 3-phase voltages of all network nodes, the symmetrical components of voltage, current and power of node 4, as well as the 3-phase currents of node 6, i.e., the node where the static load bank and the converter of the laboratory have been connected.

  Step 2. VUM is initially activated (Duration 10s). The damping susceptances Y_0 and Y_2 are set to -0.5 and -3, respectively. Afterwards, the 3-phase voltages of all network nodes, the symmetrical components of voltage, current and power of node 4, i.e., the node where the ProMiSe 3Ph4LC is located, as well as the 3-phase currents of node 6, i.e., the node where the static load bank and the converter of the laboratory have been connected, are acquired. Note that VUM remains active till the end of the experiment.

  Step 3. VR is activated (Duration 12s). Recording of the 3-phase voltages of all network nodes, the symmetrical components of voltage, current and power of node 4, i.e., the node where the ProMiSe 3Ph4LC is located, as well as the 3-phase currents of node 6, i.e., the node where the static load bank and the converter of the laboratory have been connected.

  Step 4. Modification of grid voltage levels, in order to examine the operation of the VR control scheme (Duration 10s). Recording of the 3-phase voltages of all network nodes, the symmetrical components of voltage, current and power of node 4, i.e., the node where the ProMiSe 3Ph4LC is located, as well as the 3-phase currents of node 6, i.e., the node where the static load bank and the converter of the laboratory have been connected.

  Step 5. Modification of the laboratory converter power, in order to examine the operation of the VR control scheme (Duration 16s). Recording of the 3-phase voltages of all network nodes, the symmetrical components of voltage, current and power of node 4, i.e., the node where the ProMiSe 3Ph4LC is located, as well as the 3-phase currents of node 6, i.e., the node where the static load bank and the converter of the laboratory have been connected.

  More data regarding the parameters of the Experiment 1 are provided in Tables 3-5. Here, it should be mentioned that positive active/reactive power values denote power absorption.

- **Experiment 2** (Total Duration ~22min : duration of experiment (1.5min) + data acquisition (20min)): The performance of the proposed unified strategy is evaluated in the configuration of Figure 3. The LV DN, the detailed model of a 3Ph4LC (See Figure 4) and the VR/VUM algorithms are developed in the RTDS. Note that in order to have the full model of the 3Ph4LC the 'Small time step Library' of RSCAD program has been used. **Compared to Experiment 1, in Experiment 2 the line *R/X* ratio is decreased**,

in order to demonstrate the impact of the *R/X* on the provided AS. Here, it should be highlighted that grid voltage levels as well as the power levels of load nodes have been properly readjusted to achieve similar voltage levels to POI with Experiment 1. During the experiment, the following steps have been done:

Step 1. AS remain deactivated (Duration 12s). At the beginning of the experiment an overvoltage event is observed at node 4, i.e., the node where the ProMiSe 3Ph4LC is located. Note that an overvoltage event is detected when the positive sequence voltage at the examined node exceeds 1.1pu. Recording of the 3-phase voltages of all network nodes, the symmetrical components of voltage, current and power of node 4, as well as the 3-phase currents of node 6, i.e., the node where the static load bank and the converter of the laboratory have been connected.

Step 2. VUM is initially activated (Duration 10s). The damping susceptances Y_0 and Y_2 are set to -0.5 and -1, respectively. Afterwards, the 3-phase voltages of all network nodes, the symmetrical components of voltage, current and power of node 4, i.e., the node where the ProMiSe 3Ph4LC is located, as well as the 3-phase currents of node 6, i.e., the node where the static load bank and the converter of the laboratory have been connected, are acquired. Note that VUM remains active till the end of the experiment.

Step 3. Modification of Y_2 of VUM algorithm (Duration 10s). The damping susceptances Y_2 is modified from -1 to -3, in order to demonstrate the performance of the employed VUM algorithm. Afterwards, the 3-phase voltages of all network nodes, the symmetrical components of voltage, current and power of node 4, i.e., the node where the ProMiSe 3Ph4LC is located, as well as the 3-phase currents of node 6, i.e., the node where the static load bank and the converter of the laboratory have been connected, are acquired. Note that $Y_2 = -3$ till the end of the experiment.

Step 4. Modification of Y_0 of VUM algorithm (Duration 10s). The damping susceptances Y_0 is modified from -0.5 to -0.9, in order to demonstrate the performance of the employed VUM algorithm. Afterwards, the 3-phase voltages of all network nodes, the symmetrical components of voltage, current and power of node 4, i.e., the node where the ProMiSe 3Ph4LC is located, as well as the 3-phase currents of node 6, i.e., the node where the static load bank and the converter of the laboratory have been connected, are acquired. Note that $Y_0 = -0.9$ till the end of the experiment.

Step 5. VR is activated (Duration 15s). Recording of the 3-phase voltages of all network nodes, the symmetrical components of voltage, current and power of node 4, i.e., the node where the ProMiSe 3Ph4LC is located, as well as the 3-phase currents of node 6, i.e., the node where the static load bank and the converter of the laboratory have been connected.

Step 6. Modification of grid voltage levels, in order to examine the operation of the VR control scheme (Duration 15s). Recording of the 3-phase voltages of all network nodes, the symmetrical components of voltage, current and power of node 4, i.e., the node where the ProMiSe 3Ph4LC is located, as well as the 3-phase currents of node 6, i.e., the node where the static load bank and the converter of the laboratory have been connected.

Step 7. Modification of the laboratory converter power, in order to examine the operation of the VR control scheme (Duration 16s). Recording of the 3-phase voltages of all network nodes, the symmetrical components of voltage, current and power of node 4, i.e., the node where the ProMiSe 3Ph4LC is located, as well as the 3-phase currents of node 6, i.e., the node where the static load bank and the converter of the laboratory have been connected.

More data regarding the parameters of the Experiment 2 are provided in Tables 3, 6 and 7. Here, it should be mentioned that positive active/reactive power values denote power absorption.

- **Experiment 3** (Total Duration ~17min: duration of experiment (1.5min) + duration of data acquisition (15min)): The performance of the proposed unified strategy is evaluated in the configuration of Figure 3. The LV DN and the VR/VUM algorithms are developed in the RTDS. **Compared to Experiment 1, in Experiment 3 the detailed model of the ProMiSe 3Ph4LC (See Figure 4) has been replaced with controllable current sources. Note that the filter has been remained in the analysis.** Here, it should be highlighted that grid voltage levels have been properly readjusted to achieve similar voltage levels to POI with Experiment 1. In addition, due to a resonance problem observed during the test between the lab equipment and the virtual network in RSCAD, the filter parameters are readjusted to overcome the problem. During the experiment, the following steps have been done:

  Step 1. AS remain deactivated (Duration 18s). At the beginning of the experiment an overvoltage event is observed at node 4, i.e., the node where the ProMiSe 3Ph4LC is located. Note that an overvoltage event is detected when the positive sequence voltage at the examined node exceeds 1.1pu. Recording of the 3-phase voltages of all network nodes, the symmetrical components of voltage, current and power of node 4, as well as the 3-phase currents of node 6, i.e., the node where the static load bank and the converter of the laboratory have been connected.

  Step 2. VUM is initially activated (Duration 15s). The damping susceptances Y_0 and Y_2 are set to -0.5 and -3, respectively. Afterwards, the 3-phase voltages of all network nodes, the symmetrical components of voltage, current and power of node 4, i.e., the node where the ProMiSe 3Ph4LC is located, as well as the 3-phase currents of node 6, i.e., the node where the static load bank and the converter of the laboratory have been connected, are acquired. Note that VUM remains active till the end of the experiment.

  Step 3. VR is activated (Duration 15s). Recording of the 3-phase voltages of all network nodes, the symmetrical components of voltage, current and power of node 4, i.e., the node where the ProMiSe 3Ph4LC is located, as well as the 3-phase currents of node 6, i.e., the node where the static load bank and the converter of the laboratory have been connected.

  Step 4. Modification of grid voltage levels, in order to examine the operation of the VR control scheme (Duration 15s). Recording of the 3-phase voltages of all network nodes, the symmetrical components of voltage, current and power of node 4, i.e., the node where the ProMiSe 3Ph4LC is located, as well as the 3-phase currents of node 6, i.e., the node where the static load bank and the converter of the laboratory have been connected.

  Step 5. Modification of the laboratory converter power, in order to examine the operation of the VR control scheme (Duration 16s). Recording of the 3-phase voltages of all network nodes, the symmetrical components of voltage, current and power of node 4, i.e., the node where the ProMiSe 3Ph4LC is located, as well as the 3-phase currents of node 6, i.e., the node where the static load bank and the converter of the laboratory have been connected.

  More data regarding the parameters of the Experiment 3 are provided in Tables 5, 8 and 9. Here, it should be mentioned that positive active/reactive power values denote power absorption.

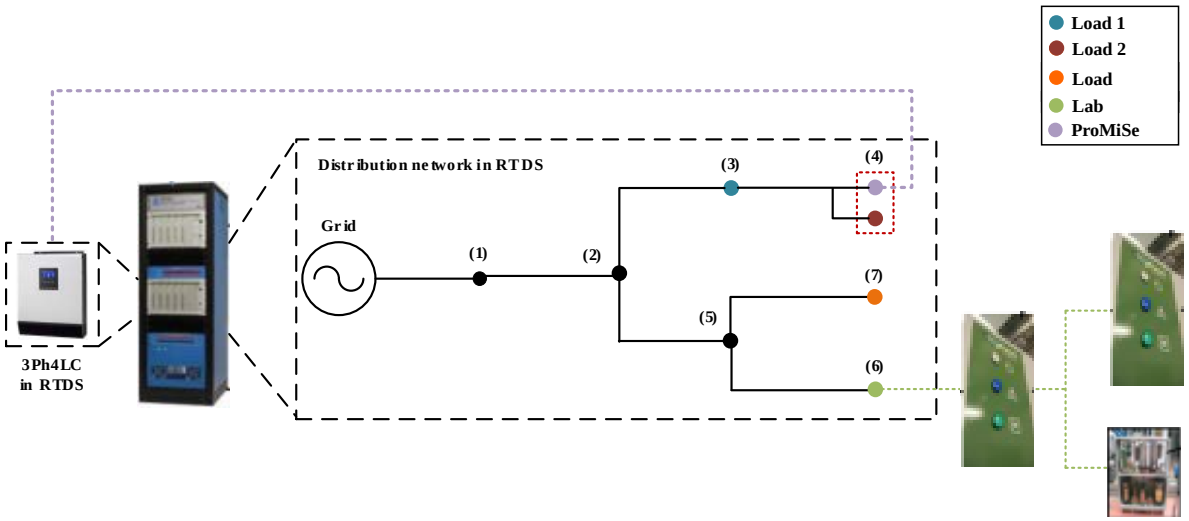

Figure 3: LV DN experimental configuration.

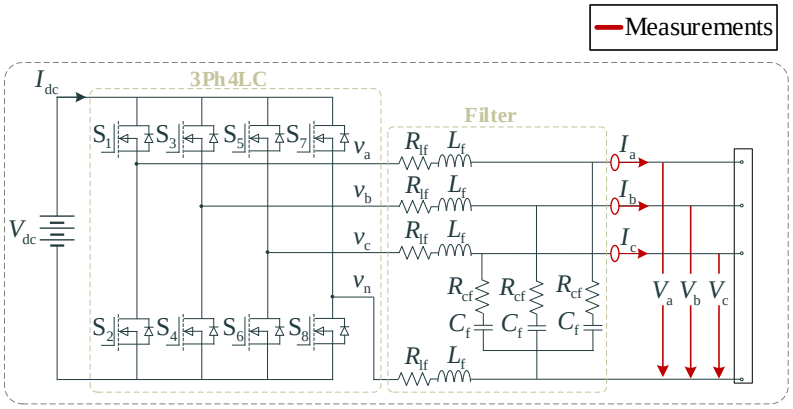

Figure 4: ProMiSe 3Ph4LC Circuit Diagram

Table 3: Parameters of Experiments 1 and 2– ProMiSe 3Ph4LC Data

Voltage of dc source		900 V
ProMiSe Converter	Apparent Power	5 kVA
	Nominal Power Factror	0.9
Filter	R_{lf}	1 mΩ
	L_{lf}	3 mH
	R_{cf}	0.15 Ω
	C_f	20 uF

Table 4: Parameters of Experiment 1 – LV DN Data

Grid Data	V_1	244.51 V
	V_2	4 % of V1
	V_0	1 % of V1
	V_1 (after Step 4)	242.77 V
Line Parameters	*R*	1.257 Ω/km
	X	0.085 Ω/km

Table 5: Parameters of Experiments 1 and 3 – Load Nodes Data

Load Name	**Phases**	**Type**	**Power Injection/Absorption**	
Load 1	3	Constant Power	Active Power	-15 kW
			Reactive Power	2.5 kVar
Load 2	3	Constant Power	Active Power	-8 kW
			Reactive Power	1.5 kVar
Load 3	1	Constant Impedance	Active Power	4.5 kW
			Reactive Power	1.333 kVar
Lab Static Load Bank	3	Constant Impedance	Active Power	8.562 kW
			Reactive Power	2.824 kVar
Lab Converter	3	Constant Power	Active Power	-4 kW
			Reactive Power	0
			Active Power (after Step 5)	-0.5 kW
			Reactive Power (after Step 5)	0

Table 6: Parameters of Experiment 2 – LV DN Data

Grid Data	V_1	245.08 V
	V_2	3.7 % of V_1
	V_0	0 % of V_1
	V_1 (after Step 6)	243.35 V
Line Parameters	*R*	0.868 Ω/km
	X	0.092 Ω/km

Table 7: Parameters of Experiment 2 – Load Nodes Data

Load Name	**Phases**	**Type**	**Power Injection/Absorption**	
Load 1	3	Constant Power	Active Power	-20 kW
			Reactive Power	1.995 kVar
Load 2	3	Constant Power	Active Power	-8.7 kW
			Reactive Power	1.5 kVar
Load 3	1	Constant Impedance	Active Power	4.5 kW
			Reactive Power	1.333 kVar
Lab Static Load Bank	3	Constant Impedance	Active Power	8.562 kW
			Reactive Power	2.824 kVar
Lab Converter	3	Constant Power	Active Power	-4 kW
			Reactive Power	0
			Active Power (after Step 7)	-0.5 kW
			Reactive Power (after Step 7)	0

Table 8: Parameters of Experiment 3 – Filter Data

Filter	R_{lf}	1 mΩ
	L_{lf}	20 mH
	R_{cf}	10 Ω
	C_f	20 uF

Table 9: Parameters of Experiment 3 – LV DN Data

Grid Data	V_1	239.31 V
	V_2	4 % of V_1
	V_0	1 % of V_1
	V_1 (after Step 6)	237.58 V
Line Parameters	*R*	1.257 Ω/km
	X	0.085 Ω/km

4 Results and Conclusions

4.1 Discussion of Results

In this section, the main results of ProMiSe are summarized.

Remark 1: The proposed unified control strategy can effectively tackle voltage violation events,

and

Remark 2:The proposed unified control strategy fully exploits the reactive power capability of DRES/DBES converters to reduce the use of active power either curtailed at DRESs or stored at DBESs.

In particular, at the beginning of all experiments it is assumed that an overvoltage problem occurs. The following analysis is related to Experiment 1, but similar remarks are also drawn for the rest experiments. From Figure 5 it can be seen that till time instant t = 22 s, voltage V_1 exceeds the maximum permissible voltage limit, i.e., 1.1 pu. Afterwards, as VR algorithm is activated (Step 3), it is shown that V_1 is decreased (See Figure 5), due to the reactive power absorption (Q_1) (negative sign) from the 3Ph4LC as verified from Figure 6. The reactive power absorption increases, since it will acquire the maximum possible value at time instant t = 25 s. It should be noted that the active power (P_1) of the 3Ph4LC remains 0 until time instant t = 25.2 s, since the VR algorithm prioritizes the use of the available reactive power. From Figure 6 it can be observed that the absorption of the maximum possible amount of reactive power it is not enough for efficient voltage regulation (V_1) within the permissible limits. Therefore, at time instant t = 25.2 s the 3Ph4LC starts absorbing active power (P_1) (negative sign) to regulate the overvoltage. This can be seen in Figure 6, where the increase of the amount of active power (P_1) increases. Moreover, from Figure 6 it is verified that as the absorbed active power (P_1) increases, the amount of the absorbed reactive power is adjusted, in order to avoid violations regarding the operational characteristics of the 3Ph4LC. As the simulation procedure proceeds, from Figure 5 it can be easily realized that voltage (V_1) is regulated within the permissible limits at time instant t = 28.63 s. In order to maintain voltage (V_1) within permissible limits the 3Ph4LC continues to absorb the amounts of reactive (Q_1) and active power (P_1), which have been determined from the VR control, until a change in the grid voltage levels occurs. At time instant t = 34 s a change in the operational conditions of the grid occurs, which leads to a voltage (V_1) decrease below the desirable dead band (Step 4). In particular, in Figure 6 the reduction of the active power (P_1) and the readjustment the reactive power (Q_1) of the 3Ph4LC is presented, till voltage (V_1) is regulated in the desirable deadband (See Figure 5), in order to prevent the unnecessary absorption of active (P_1) and reactive power (Q_1). The 3Ph4LC continues to absorb the new amounts of reactive (Q_1) and active power (P_1), until a change in the power of the Lab converter occurs at time instant t = 44 s, which leads to a voltage (V_1) decrease below the desirable dead band again (Step 5). Once again, in Figure 6 the reduction of the active power (P_1) is depicted, but since the voltage (V_1) at the POI has not been regulated and the active power (P_1) is zero, the reactive power (Q_1) starts decreasing, till voltage (V_1) is regulated at time instant t = 49 s. After voltage has been successfully regulated (V_1), the control process is deactivated and the 3Ph4LC absorbs only the required amount of reactive power (Q_1) to maintain voltage (V_1) within permissible limits.

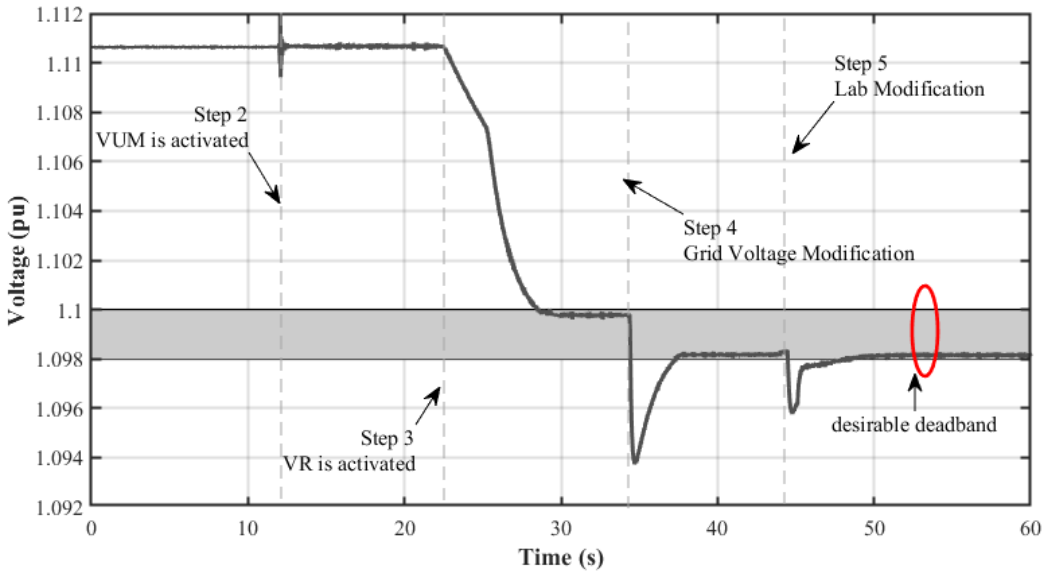

Figure 5: Positive-Sequence Voltage at POI during Experiment 1

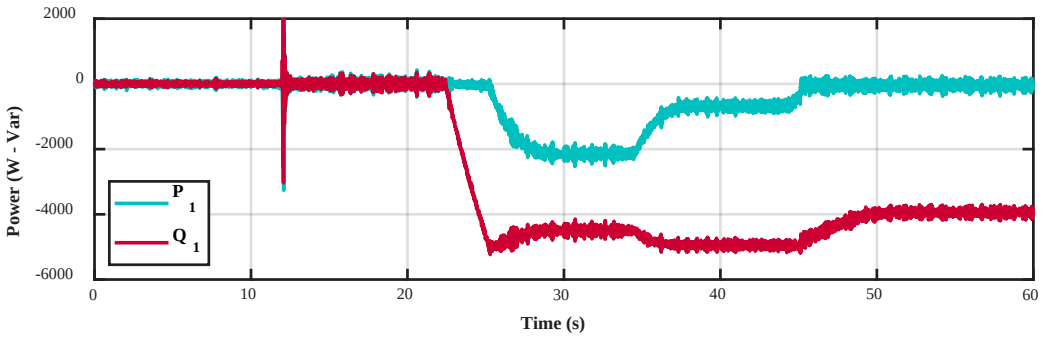

Figure 6: Positive-Sequence Active and Reactive Power of ProMiSe 3Ph4LC during Experiment 1

Remark 3: The employed VR and VUM algorithms are fully decoupled

The following analysis is related to Experiment 3, but similar remarks are also drawn for the rest experiments. In particular, from Figure 7(b) and 7(c) it is shown that VUM is activated at time instant t = 18 s (Step 2), where also an increase of negative- and zero-sequence reactive power (Q_2, Q_0) absorption (negative sign) of the 3Ph4LC is observed. This increase leads to a reduction of voltages in the negative (V_2) and in zero (V_0) sequence, thus reducing the unbalance, as is verified from Figure 8(b) and 8(c). Moreover, from Figure 7 (b) and 7(c) it is verified that reactive power acts as the only means of unbalance mitigation, since during the Experiment the active power of the negative (P_2) and of zero (P_0) sequence remains zero. Additionally, according to Figures 7 and 8, it can be seen that the activation of VR control sceme does not influence the VUM control verifying that the two employed algorithms are fully decoupled.

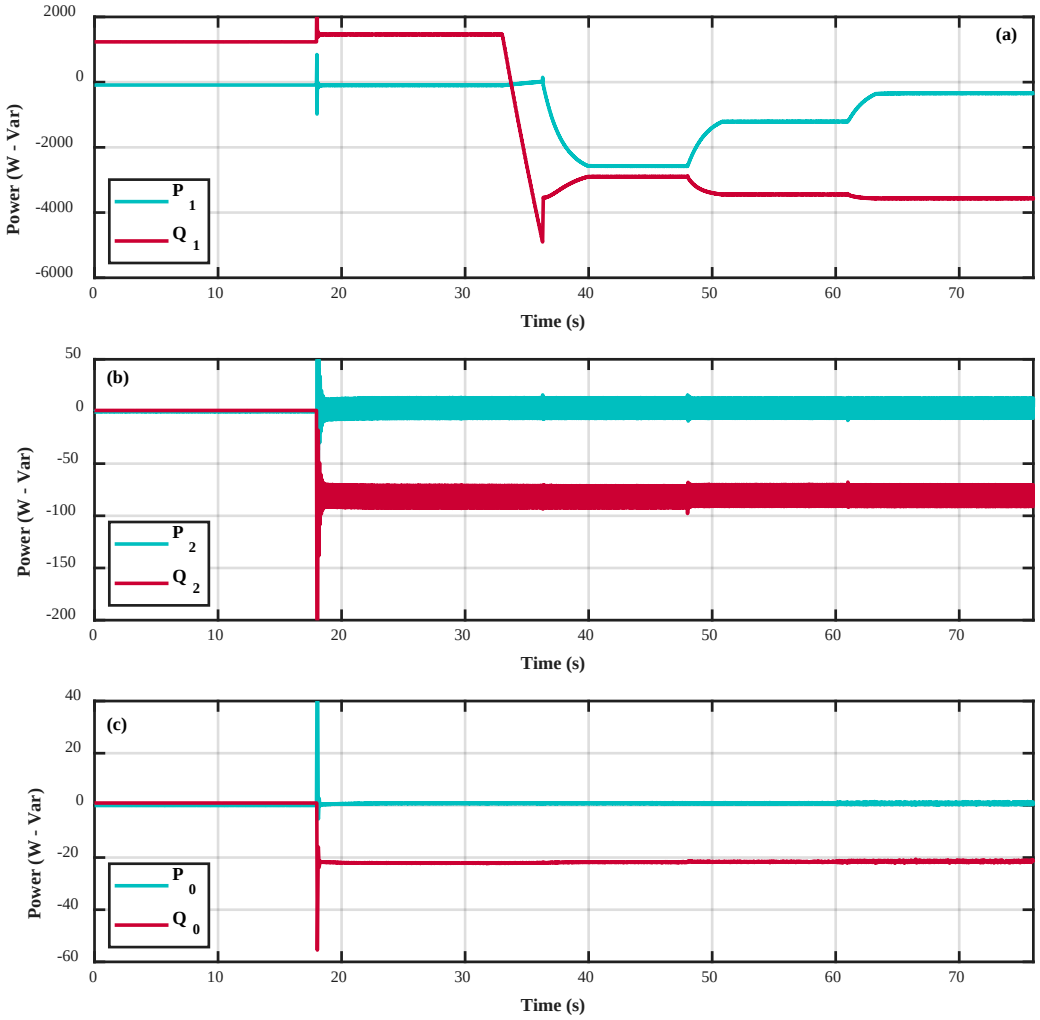

Figure 7: (a) Positive-, (b) Negative- and (c) Zero-Sequence Active and Reactive Power of ProMiSe 3Ph4LC during Experiment 3

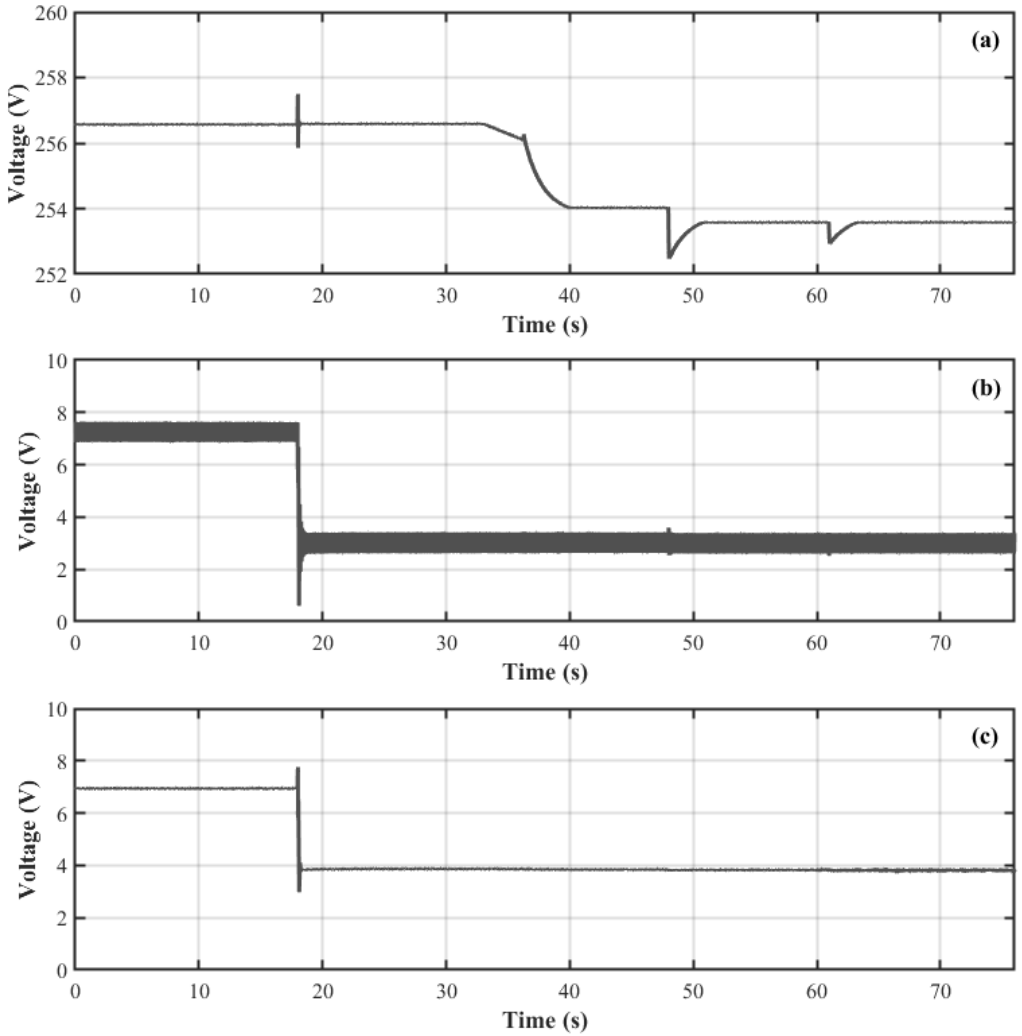

Figure 8: (a) Positive-, (b) Negative- and (c) Zero-Sequence Voltage at POI of the ProMiSe 3Ph4LC during Experiment 3

Remark 4: The proposed unified control strategy can be effectively employed by 3Ph4LC located at grids with different *R/X* Line ratio

By comparing the obtained results of Experiments 1 and 2, where the 3Ph4LC is located in LV DNs presenting different *R/X* line ratios, i.e., 14.79 and 9.43 for Experiment 1 ad 2, respectively, it can be realized that the provision of AS by the proposed unified control strategy is achieved in both experiments. In particular, from Figure 9, it is verified that voltage violation events can be effectively tackled in both experiments. In addition, for the conducted modifications the operation of the proposed unified control strategy remains similar in both cases. Nevertheless, it should be highlighted that in order to achieve similar performance in both experiments, different active/reactive power should be absorbed by the 3Ph4LC, as shown in Figure 10. Specifically, by comparing Figures 10(a) and 10(b), it can be realized, that when the 3Ph4LC is installed in LV DNs presenting lower *R/X* line ratio should absorb higher amount of active/reactive power, in order to achieve similar VR as the corresponding 3Ph4LC located in a LV DN with higher *R/X* line ratio.

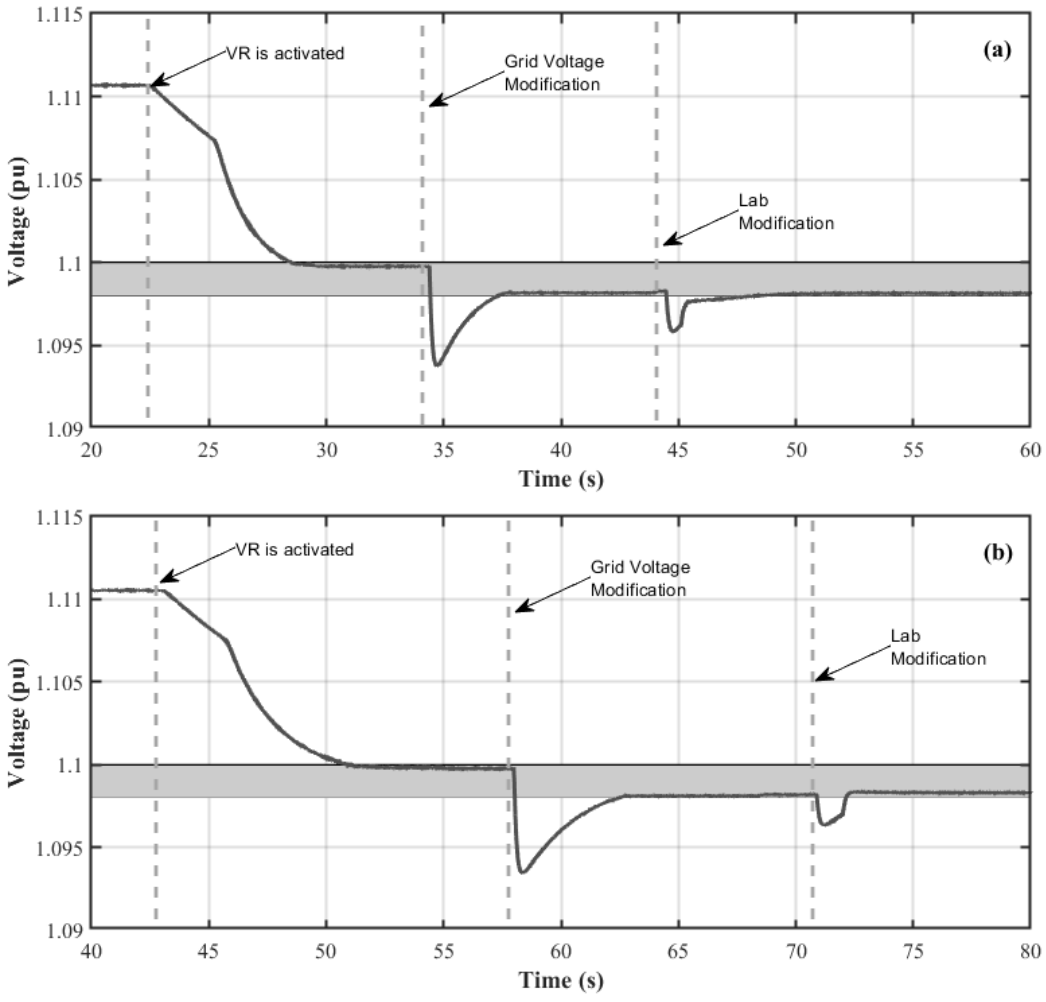

Figure 9: Positive-Sequence Voltage at POI during (a) Experiment 1 and (b) Experiment 2

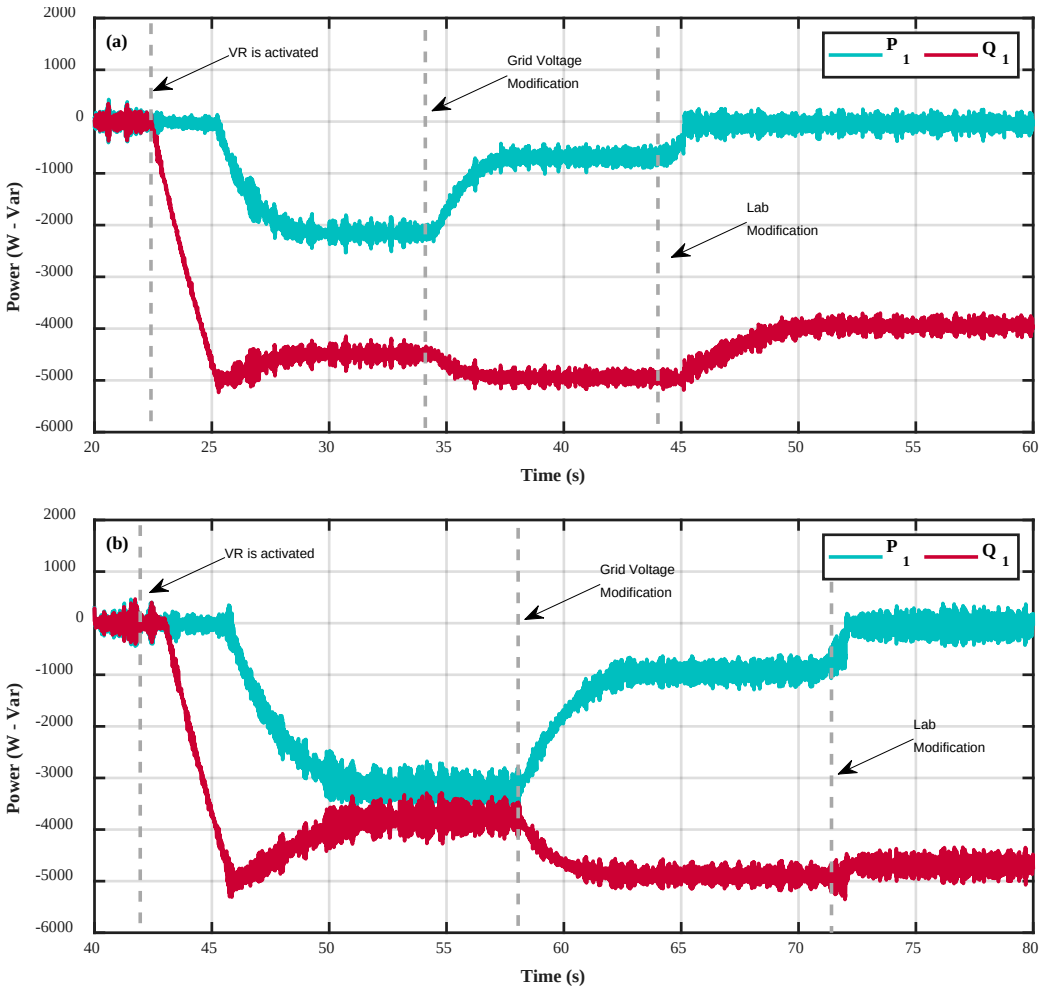

Figure 10: Positive-Sequence Active and Reactive Power of ProMiSe 3Ph4LC during (a) Experiment 1 and (b) Experiment 2

Remark 5: By readjusting the damping susceptance of the negative- and zero-sequence the unbalance levels can be further improved

In Figure 11, the effect of different damping susceptance values on the negative-(V_2) and zero-(V_0) sequence voltage levels is assessed. In particular, at the beginning of the experiment the voltage unbalance is 3.01% and 2.63% for the negative- and zero-sequence, respectively. At time instant t = 12 s (Step 2 of Experiment 2), it can be seen that the activation of VUM considering a Y_2 = -1j and a Y_0 = -0.5j, the voltage unbalance levels for the negative- and zero-sequence voltages are reduced to 2.47% and 1.74%, respectively. To be in compliant with the existing standards that foresee that the negative-sequence voltage levels should be below 2%, at time instant t = 22 s (Step 3 of Experiment 2), Y_2 is modified to -3j, to achieve even better unbalance levels. Indeed, this modification leads to a further decrease of negative-sequence voltage unbalance levels (1.5%). Afterwards, at time instant t = 32 s (Step 4 of Experiment 2), Y_0 is also modified to -0.9j, to better improve unbalance levels of zero-sequence (1.2%).

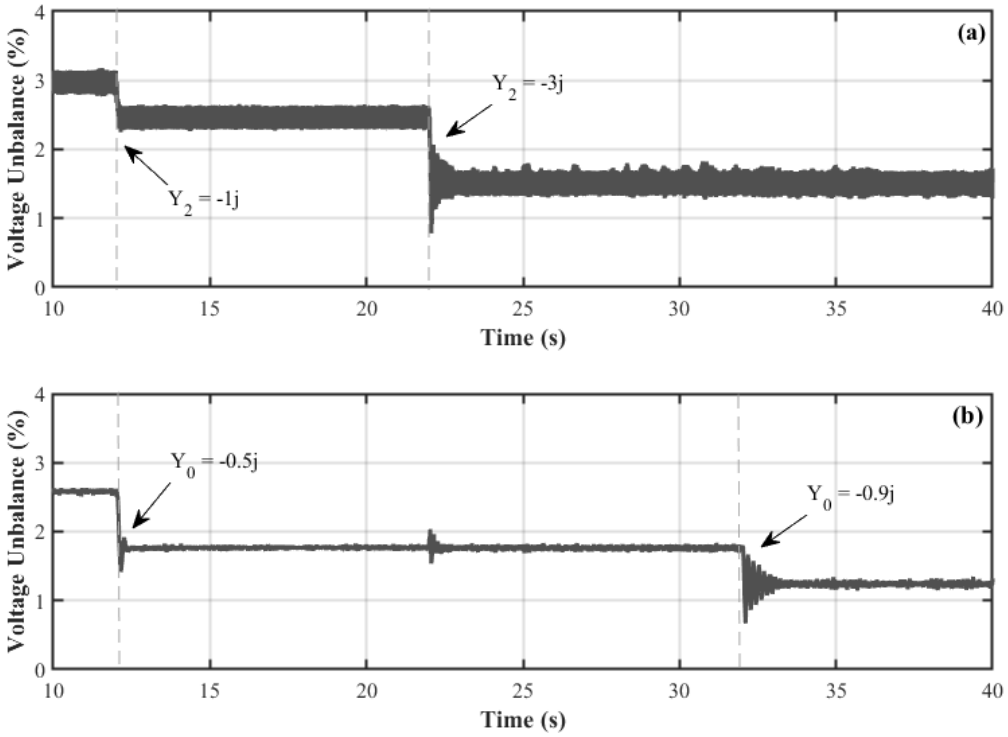

Figure 11: (a) Negative- and (b) Zero-Sequence Voltage Unbalance at POI of the ProMiSe 3Ph4LC for different damping susceptance values

4.2 Conclusions

The main conclusions of ProMiSe can be summarized as:

- The proposed unified control strategy can effectively tackle voltage violation events.
- The proposed unified control strategy fully exploits the reactive power capability of DRES/DBES converters to reduce the use of active power either curtailed at DRESs or stored at DBESs.
- The employed VR and VUM algorithms are fully decoupled. Unlike the most relevant control schemes, the proposed VUM and VR algorithms are decoupled, removing this way any interference among them and subsequently facilitating their accurate and efficient handling. In particular, the VR method regulates the positive sequence voltages and currents, respectively, while the VUM algorithm aims to reduce the zero- and the negative-sequence voltages.
- The proposed unified control strategy can be effectively employed by 3Ph4LC located at grids with different *R/X* Line ratio
- By readjusting the damping susceptance of the negative- and zero-sequence the unbalance levels can be further improved
- Introduction of the damping susceptance. Contrary to the damping conductance concept that utilizes the active power as the main means for VUM, a damping susceptance is introduced within the proposed VUM method allowing the exploitation and control of the reactive power.
- A detailed 3Ph4LC model with the necessary control units has been developed in RSCAD program and it can be used in future projects in order to evaluate the performance of different AS.
- The detailed 3Ph4LC model with the necessary control units necessitate increased computational power.
- During the PHiL experiments, resonance issues between the virtual and the physical equipment can emerge, for this reason the configurations should be properly readjusted.
- The members of the research group have been trained and acquired expertise on measuring, data recording and analysis, developing models in PHiL, etc.
- Results and proposed methods will be presented in one scientific conference and will be published in one journal paper.

5 Open Issues and Suggestions for Improvements

In the future the following improvements can be made:

- Active power smoothing algorithms and congestion management control schemes can be implemented in the proposed unified control strategy of ProMiSe, to assess the provision of more AS.
- The performance of the ProMiSe 3Ph4LC can be evaluated in more complex network configurations, e.g., DNs with increased number of nodes or DNs equipped with multiple ProMiSe 3Ph4LCs that provide simultaneously AS.
- The scalability of the proposed control strategy to the MV grid can be evaluated by using combined HV/MV/LV grid models.
- Computational power requirements is challenging, in order to ensure that detailed models of converters in RTDS.

References

[1] D. Olivares, et al., Trends in Microgrid Control, IEEE Trans. Smart Grid 5 (4) (2014) 1905–1919.

[2] A. Saint-Pierre, et al., Active Distribution System Management: A Dual-Horizon Scheduling Framework for DSO/TSO Interface Under Uncertainty, IEEE Trans. Smart Grid 8 (5) (2017) 2186– 2197.

[3] G. Kryonidis, et al., Ancillary services in active distribution networks: A review of technological trends from operational and online analysis perspective, Renew. Sustain. Energy Rev. 147 (2021) 111198.

[4] Y. Wang, et al., Coordinated control of distributed energy-storage systems for voltage regulation in distribution networks, IEEE Trans. Power Del. 31 (3) (2016) 1132–1141.

[5] Z. Tang, et al., Distributed coordinated reactive power control for voltage regulation in distribution networks, IEEE Trans. Smart Grid 12 (1) (2021) 312–323.

[6] M. Kabir, et al., Improving voltage profile of residential distribution systems using rooftop PVs and battery energy storage systems, Applied Energy 134 (2014) 290–300.

[7] T. Mai, et al., Adaptive coordination of sequential droop control for PV inverters to mitigate voltage rise in PV-rich LV distribution networks, Electr. Power Syst. Res. 192 (2021) 106931.

[8] H. Xu, et al., Data-driven voltage regulation in radial power distribution systems, IEEE Trans. Power Syst. 35 (3) (2020) 2133–2143.

[9] S. Hashemi, et al., Efficient control of energy storage for increasing the PV hosting capacity of LV grids, IEEE Trans. Smart Grid 9 (3) (2018) 2295–2303.

[10] M. Zeraati, et al., A consensus-based cooperative control of PEV battery and PV active power curtailment for voltage regulation in distribution networks, IEEE Trans. Smart Grid 10 (1) (2019) 670–680.

[11] J. Li, et al., Distributed online var control for unbalanced distribution networks with photovoltaic generation, IEEE Trans. Smart Grid 11 (6) (2020) 4760–4772.

[12] M. Abad, et al., Photovoltaic hosting capacity sensitivity to active distribution network management, IEEE Trans. Power Syst. 36 (1) (2021) 107–117.

[13] IEEE standard for interconnection and interoperability of distributed energy resources with associated electric power systems interfaces, IEEE Std 1547-2018 (Revision of IEEE Std 1547-2003) (2018) 1–138.

[14] M. Yao, et al., Mitigating voltage unbalance using distributed solar photovoltaic inverters, IEEE Trans. Power Syst. 36 (3) (2021) 2642–2651.

[15] D. Bozalakov, et al., Overvoltage and voltage unbalance mitigation in areas with high penetration of renewable energy resources by using the modified three-phase damping control strategy, Electr. Power Syst. Res. 168 (2019) 283–294.

[16] E. Kontis, et al., A two-layer control strategy for voltage regulation of active unbalanced LV distribution networks, Int. J. Electr. Power Energy Syst. 111 (2019) 216–230.

[17] K. Pippi, et al., A unified control strategy for voltage regulation and congestion management in active distribution networks, Electr. Power Syst. Research 212 (2022) 108648.

Disclaimer

This document contains material, which is copyrighted by the authors and may not be reproduced or copied without permission.

The commercial use of any information in this document may require a licence from the proprietor of that information.

Neither the Lab Access User Group as a whole, nor any single person warrant that the information contained in this document is capable of use, nor that the use of such information is free from risk. Neither the Lab Access User Group as a whole, nor any single person accepts any liability for loss or damage suffered by any person using the information.

This document does not represent the opinion of the European Community, and the European Community is not responsible for any use that might be made of its content.

Copyright Notice

This project has received funding from the European Union's Horizon 2020 research and innovation programme under Grant Agreement No. 870620.